GEOMETRY OF QUANTUM STATE MANIFOLDS

Střeleček J.[*], Cejnar P.[†]

Institute of Particle and Nuclear Physics, Faculty of Mathematics and Physics, Charles University, V Holešovičkách 2, 180 00 Prague, Czechia

[*]strelecek@ipnp.mff.cuni.cz [†]cejnar@ipnp.mff.cuni.cz

From Fisher metric to quantum state manifolds

The space of probability distributions $p(\mathbf{\Lambda})$ for $\mathbf{\Lambda} \in \mathbb{R}^D$ can be equipped with a *Fisher information metric*. In quantum physics, we obtain probability distributions by taking $\langle A_i|\psi\rangle$ for a wave function $|\psi\rangle$ and eigenvector $|A_i\rangle$ of some observable $\hat{A}$. As a result, we get a Projective Hilbert space $\mathbb{C}P^n$ equipped with a *Fubini-study metric* [1]. Such a metric can be defined between two states $|\psi\rangle, |\varphi\rangle \in \mathbb{C}P^n$ as $\mathrm{d}s^2_{FS} \coloneqq \arccos|\langle\psi|\varphi\rangle|$. Approximating for close states, we get a Provost-Vallee (PV) metric [2]

$$\mathrm{d}s^2_{PV} = 1 - |\langle\psi|\psi + \delta\psi\rangle|^2. \tag{1}$$

As opposed to the Hilbert space with Fubini-Study metric, this creates a *length space* (the distance between any two points is not an infimum over all possible paths) only on a so-called *State manifolds*.

State manifolds

Consider a $n-$dimensional projective Hilbert space $\mathbb{C}P^n$ for $n \in \mathbb{N} \cup \{+\infty\}$, and Hamiltonian $\hat{H}(\mathbf{\Lambda})$ with *driving parameters*, denoted collectively as a vector $\mathbf{\Lambda} \in \mathbb{R}^D$. The spectrum is assumed to be bound and non-degenerate, except for a finite number of points. The Schrödinger equation then reads $\hat{H}|\psi_n(\mathbf{\Lambda})\rangle = E_n|\psi_n(\mathbf{\Lambda})\rangle$.
The mapping $\mathbf{\Lambda} \to |\psi_0(\mathbf{\Lambda})\rangle$ defines a ground state manifold (or any excited manifold analogically)

$$\mathcal{M}_0 \coloneqq \cup_{\mathbf{\Lambda}\in\mathbb{R}^D}|\psi_0(\mathbf{\Lambda})\rangle \tag{2}$$

equipped with a Geometric tensor

$$Q_{\mu\nu} \coloneqq \langle\psi_{0,\mu}|(\mathrm{Id} - |\psi_0\rangle\langle\psi_0|)|\psi_{0,\nu}\rangle, \tag{3}$$

where comma denotes a partial derivative. A pullback of a PV-metric in Eq. 1 is then $g_{\mu\nu} = \mathrm{Re}Q_{\mu\nu}$. In addition we get a symplectic form $\chi_{\mu\nu} = \mathrm{Im}Q_{\mu\nu}$.
The physical meaning of this geometry is still not fully understood. There are many special practical showcases, such as *decohering driving* [3], or quantum search algorithms [4]. Other implications for quantum state driving are still being discovered. Here we discuss its meaning in Quantum phase transitions.

Geometry of Quantum Phase Transitions

Quantum phase transitions (QPT) describe the phenomenon where the ground state (or its derivative) of a parametrically driven Hamiltonian $\hat{H}(\mathbf{\Lambda})$ changes discontinuously with the parameter $\mathbf{\Lambda}$.
From Eq. 1, we see that on QPT, the metric distance diverges. From $\mathrm{d}s^2 = g_{\mu\nu}\mathrm{d}\mathbf{\Lambda}^\mu\mathrm{d}\mathbf{\Lambda}^\nu$, we see that along QPT, the metric tensor needs to be discontinuous. Because of the summation, the converse does not hold. It is still unclear in which cases the converse implication holds and in which cases the discontinuities are reflected in the geometry of state manifolds itself, i.e. in Ricci scalar R, or when it is just a matter of a coordinate system. Schematically

$$QPT \Leftrightarrow \mathrm{d}s^2 \text{ is disc.} \Rightarrow g_{\mu\nu} \text{ is disc.} \overset{?}{\leftrightarrow} R \text{ is disc.}$$

Some studies [5], [6] show that for specific models $R = const.$ and the ground state manifold itself is smooth, meaning the discontinuities are only coordinate-ones. For other models, such as in [7], divergences occur even in the Ricci scalar.
Another topic of interest concerns the *geodesics*. It was shown that they do not cross the QPT [8]. The demonstration of their behaviour is beyond the scope of this poster, and will be presented in the article.

Fully connected multi-qubit model

We define the fully connected multi-qubit model (a special parametrization of a Lipkin model) using two real parameters $\mathbf{\Lambda} \equiv (\lambda;\chi)$ with Hamiltonian

$$\begin{aligned}\hat{H}(\lambda,\chi) &= \hat{J}_3 + \lambda\hat{V}_1 + \chi\hat{V}_2 + \chi^2\hat{V}_3,\\ \hat{V}_1 &\coloneqq -\frac{1}{2j}\hat{J}_1^2,\\ \hat{V}_2 &\coloneqq -\frac{1}{2j}\left[\hat{J}_1(\hat{J}_3 + j\mathrm{Id}) + (\hat{J}_3 + j\mathrm{Id})\hat{J}_1\right],\\ \hat{V}_3 &\coloneqq -\frac{1}{2j}(\hat{J}_3 + j\mathrm{Id})^2,\end{aligned} \tag{4}$$

for the *angular momentum operator* $\hat{\boldsymbol{J}} \equiv (\hat{J}_1, \hat{J}_2, \hat{J}_3)^T$. In further discussion, we use the maximal $j = N/2$. The phase structure of this model is shown in Fig. 1.

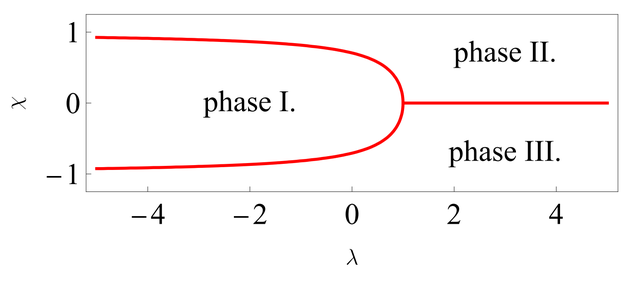

Fig. 1: Phase structure for a multi-qubit model.

The metric tensor elements for $N = 5$ are shown in Fig. 2. With increasing N it converges to the classical limit displayed on the right. The QPT emerges from two phenomena. First, for $\lambda < 0$, the number of diabolic points (points of spectrum degeneracy) increases with N. Abrupt changes in the ground state connect these points, and for $N \to \infty$ they cover the whole separatrix in this area. Second, different phenomena occur on the χ axis, where the discontinuity is created as the "valley" going along the axis sharpens, creating the discontinuity in derivative at the classical limit. These two areas are connected by a fast-changing ground state, leading to a discontinuity in the classical limit along the whole separatrix.

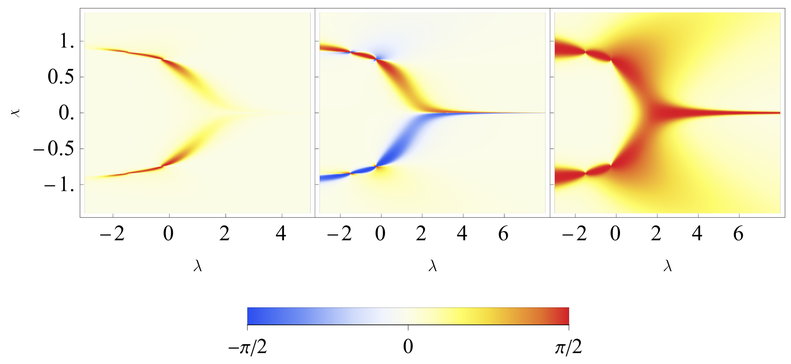

Fig. 2: Metric tensor elements for $N = 5$ multi-qubit model. From left $\arctan g_{\lambda\lambda}$, $\arctan g_{\lambda\chi}$, $\arctan g_{\chi\chi}$.

Lipkin model, Classical limit

As a classical limit, we calculated the Hartree-Bose condensate. Generally, we search for the $N-$particle condensate ground state ($\hat{N} = \hat{t}^+\hat{t} + \hat{s}^+\hat{s}$) for two types of bosons, by exciting bosonic vacuum $|0\rangle$ as

$$|\psi_{HB}(\mathbf{\Lambda})\rangle = \frac{1}{\sqrt{N!}}[\hat{B}^+]^N|0\rangle\,,\ \hat{B}^+ \coloneqq \frac{\tau(\mathbf{\Lambda})\hat{t}^+ + \hat{s}^+}{\sqrt{1+|\tau(\mathbf{\Lambda})|^2}} \tag{5}$$

The ground state $|\psi_{HB}\rangle$ can be found by minimizing the function $\epsilon(\tau(\mathbf{\Lambda})) \coloneqq \langle\psi_{HB}|\hat{H}_{HB}|\psi_{HB}\rangle$ with respect to τ. $\hat{H}_{HB}$ is a Hartree-Bose hamiltonian derived from Eq. 4. As a result, we get $\tau = \mathrm{Re}\,\tau = \tau(\lambda,\chi)$, shown in Fig. 3. Discontinuities in this plot correspond to QPTs. Metric tensor elements are then

$$g_{\mu\nu} = \mathcal{N}\begin{pmatrix}\tau_{,\lambda}^2 & \tau_{,\lambda}\tau_{,\chi}\\ \tau_{,\lambda}\tau_{,\chi} & \tau_{,\chi}^2\end{pmatrix} \tag{6}$$

for $\mathcal{N} \coloneqq N/(1+\tau^2)^2$. The determinant of such a metric is identically zero. The ground state manifold metric tensor elements (see Fig. 4) are linear with N. Except for QPTs, additional discontinuities are being created along lines $\mathrm{d}\tau/\mathrm{d}\lambda = 0$ at the classical limit. This supports the statement that along QPT, components $g_{\mu\nu}$ must contain discontinuity, but a discontinuity in the metric tensor component does not necessarily imply the existence of QPT.

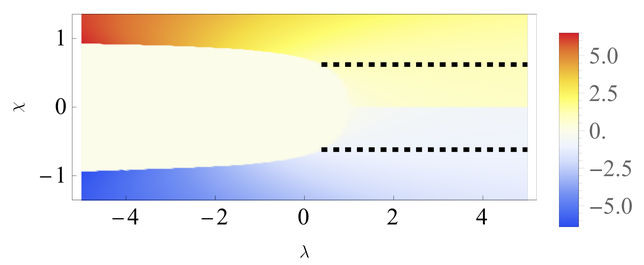

Fig. 3: Value of $\tau(\lambda,\chi)$ in Hartree-Bose condensate of a multi-qubit model. Black, dashed lines correspond to $\mathrm{d}\tau/\mathrm{d}\lambda = 0$.

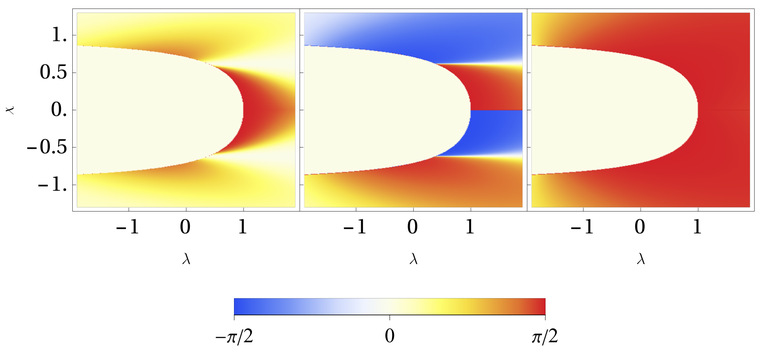

Fig. 4: Metric tensor for a Hartree-Bose condensate for $N = 100$. From left: $\arctan g_{\lambda\lambda}$, $\arctan g_{\lambda\chi}$, $\arctan g_{\chi\chi}$

Conclusions

We have shown that QPT leads to metric tensor discontinuities, but the converse does not generally hold. This is supported by a specific numerical model, for which we semi-analytically found the classical limit of the metric tensor. The emergence of QPT from a finite-dimensional model was presented and explained by two phenomena – the connection of diabolic points and the "sharpening" of the wave function parametric dependence.

The work is supported by Charles University GA UK 2023 No. 207723.

References

[1] Cheng R. Quantum geometric tensor (fubini-study metric) in simple quantum system: A pedagogical introduction. *arXiv:1012.1337v2*, 2010.

[2] J. P. Provost and Vallee G. Riemannian structure on manifolds of quantum states. *Communications in Mathematical Physics*, 76:289–301, 1980.

[3] Cejnar P., Stránský P., Střeleček J., and Matus F. Decoherence-assisted quantum driving. *Phys. Rev. A*, 107:L030603, 2022.

[4] Cafaro C., Ray S., and Alsing P. M. Geometric aspects of analog quantum search evolutions. *Phys. Rev. A*, 102:052607, 2020.

[5] Gutiérrez-Ruiz D., Diego Gonzalez, Chávez-Carlos J., Hirsch J. G., and J. D. Vergara. Quantum geometric tensor and quantum phase transitions in the Lipkin-Meshkov-Glick model. *Phys. Rev. B*, 103:174104, 2021.

[6] Gutiérrez-Ruiz D., Chávez-Carlos J., Gonzalez D., Hirsch J. G., and J. D. Vergara. Quantum metric tensor of the Dicke model: Analytical and numerical study. *Phys. Rev. B*, 105: 214106, 2022.

[7] Zanardi P., Giorda P., and Cozzini M. Information-theoretic differential geometry of quantum phase transitions. *Phys. Rev. L*, 99:100603, 2007.

[8] Kumar P., Mahapatra S., Phukon P., and Sarkar T. Geodesics in information geometry: Classical and quantum phase transitions. *Phys. Rev. E*, 86:051117, 2012.

FACULTY OF MATHEMATICS AND PHYSICS Charles University